http://dx.doi.org/10.17159/2411-9717/2016/v116n1a6

Response surface optimization of process parameters for the removal of F and Cl from zinc oxide fume by microwave sulphating roasting

by T. Hu*†‡, Z. Li*†‡, C. Liu*✦, L. Zhang*†‡, J. Peng*†‡✦, and B. Wang*†‡

Synopsis

Microwave sulphating roasting was applied to zinc oxide fume from a fuming furnace for the removal of F and Cl. The effect of important parameters such as roasting temperature, holding time. and vapour flow were investigated and the process conditions were optimized using response surface methodology. The results showed that the effects of roasting temperature and holding time on the removal efficiency of F and Cl were most significant, and the effect of vapour flow is of much lower importance. The defluorination and dechlorination efficiency increased rapidly as the roasting temperature and holding time increased, while the vapour flow had little effect. The defluorination efficiency could reach 91.3% while the dechlorination efficiency could reach 89.5%, under the process conditions of roasting temperature 655°C, holding time 65.2 minutes, and vapour flow of 6.8 ml/min. The results showed that the removal of F and Cl from zinc oxide fume using a microwave direct roasting process is feasible and reliable.

Keywords

zinc oxide fume, microwave sulphating roast, removal of F and Cl, response surface methodology.

Introduction

Zinc is one of the most important metals, which is required for various applications in the metallurgical, chemical, and textile industries. The depletion of high-grade ores of zinc and the accumulation of large quantities of metallic scrap, as well as metallurgical wastes, have led to a significant interest in processing these zinc secondary sources (Vahidi *et al.*, 2009; Dakhili *et al.*, 2011; Li *et al.*, 2012). Zinc secondary materials such as zinc ash, dross, flue dusts, sludge, and residues are generated in various chemical and metallurgical industries (Agrawal *et al.*, 2004; Sahu *et al.*, 2004; Jha *et al.*, 2001). Although the recovery of zinc from various secondary sources brings huge economic and environmental benefits, impurities result in decreasing recycling rates for these materials. In particular, the electrowinning of zinc is strongly influenced by chlorine and fluorine, which cause anode corrosion and sticking of zinc metal on the cathode (Lashgari and Hosseini, 2013; Güresin and Topkaya, 1998). F and Cl ions in electrolytes have to be removed first to meet the requirements for zinc electrowinning (F < 80 mg/L, Cl < 100 mg/L) (Cinar Sahin *et al.*, 2000; Lan *et al.*, 2006).

The conventional pyrometallugical processes to remove F and Cl are based on the volatilization of these low boiling-point and volatile halides. Lead and zinc chloride show high vapour pressures and low boiling points at relatively low temperature (Cinar Sahin *et al.*, 2000; Wang *et al.*, 2007). At elevated temperatures the halides convert to a vapour phase, enabling their removal from the solid matrix. In the conventional roasting process, zinc oxide fume is roasted in excess of 700°C for an extended time to volatilize the halides, but the removal efficiency is low (Barakat, 2003). Recently, the raw materials for zinc smelting have become more complex and the F and Cl contents in the residues are also increasing, creating many challenges for the multiple hearth furnace and fuming furnace, resulting in a low removal efficiency of F and Cl (Zeng *et al.*, 2007). This necessitates the development of better processes for the removal of F and Cl.

Based on the thermodynamic analysis of volatilization reactions, thermal hydrolysis and sulphate reactions of halides are viable. In the

* *National Local Joint Laboratory of Engineering Application of Microwave Energy and Equipment Technology, Kunming, China.*

† *CKey Laboratory of Unconventional Metallurgy, Ministry of Education, China.*

‡ *Faculty of Metallurgy and Energy Engineering, Kunming University of Science and Technology, China*

✦ *Faculty of Chemistry and Environment, Yunnan Minzu University.*

 ISSN 2225-6253. Paper received Jul. 2014; revised paper received Sep. 2015.

present work, the microwave sulphating roasting process was applied to remove F and Cl from zinc oxide fume, with the advantages of rapid and selective microwave heating. The roasting temperature, holding time, and air and steam flow were selected as the independent variables to test their effect on defluorination and dechlorination efficiency of zinc oxide fume. Response surface methodology (RSM) based on the central composite design (CCD) was employed to determine the optimal conditions, and a quadratic model correlating the removal efficiency of F and Cl to the three variables was then developed.

Materials and methods

Experimental materials

The zinc oxide fume used in the experiments was received from a fuming furnace smelting process in Yunnan Province in China. The chemical composition of the zinc oxide dust is listed in Table I. The zinc oxide fume contains high Zn and Pb contents, which are of significant economic value. F and Cl in the zinc oxide fume may be incorporated into the leaching solution during the zinc leaching process, resulting in excessive F and Cl concentrations, which is a serious issue in the zinc electrolysis process. Additionally, the S content is 3.84%, which provides the necessary reactant for sulphating roasting.

Experimental set-up and method

The main experimental equipment was a 3 kW box-type microwave reactor designed by the Key Laboratory of Unconventional Metallurgy, Kunming University of Science and Technology. A schematic of the experimental set-up is shown in Figure 1.

The experimental facilities comprised a microwave reactor, air inlet into the system, a stirring device, and an off-gas absorption system. Firstly, 300 g of sample was dried, ground, and placed in the mullite crucible, which was surrounded with heat insulation materials. The crucible was then transferred into the microwave reactor and heated at a microwave frequency of 2450 MHz and power of 0 kW to 3 kW, which could provide continuous adjustable and automatic temperature control. The mullite crucible had a diameter of 90 mm and a height of 120 mm, with a strong transparent wave performance and good thermal shock resistance. The temperature measuring device was a shielded sleeve thermocouple that could measure up to 1300°C. Before starting an experiment, the microwave, stirring, and off-gas absorption systems were switched on. The off-gas absorption system was developed to collect and absorb the flue dust. This off-gas system consisted of a buffer bottle, two water absorption bottles, an alkali absorption bottle, and a micro suction pump. The test equipment also had a stirring device, and the stirring speed ranged from 0 to 160 r/min to meet the required zinc oxide dust-stirring intensity. The stirring system enhanced the reactions by enabling the release of fluoride and chloride compounds. In this sulphating roasting, the stirring speed was set at 120 r/min. In each test the material was microwave-roasted while water vapour carried by the air flow passed into the reactor after the material was heated to the set roasting temperature. Reaction gases could be introduced via a rotameter and a mini air compressor pump, controlling the flow rate of air or water vapour. After a predetermined roasting time, the samples were taken out and cooled at ambient temperature in air. The fluorine ion-selective electrode and the silver chloride turbidimetric

Table

Chemical composition of zinc oxide dust sample (mass percentage)

Zn	Pb	Ge	Cd	Fe	Sb	S	As	F	Cl	SiO_2	CaO
53.17	22.38	0.048	0.21	0.38	0.23	3.84	1.04	0.0874	0.0783	0.65	0.096

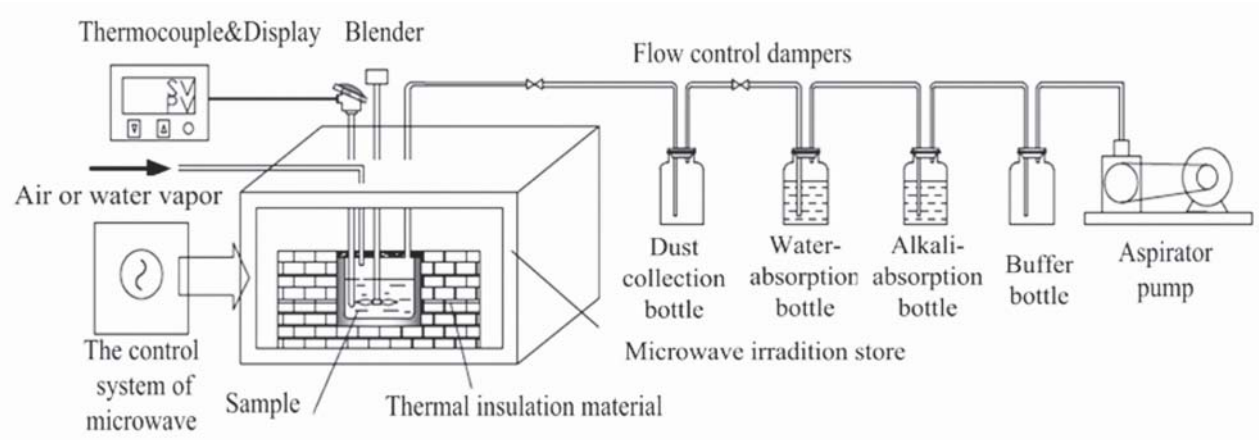

Figure 1—Connection diagram of microwave roasting experiment equipment

method (d'Heilly *et al.*, 2007; Zenki and Iwadou, 2002) were used for the determination of the fluorine and chlorine content. The initial raw materials contained levels of 166.3 mg/L fluorine and 145.4 mg/L chlorine.

The fluorine and chlorine removal efficiencies were mathematically expressed as

$$\eta = \frac{M - M'}{M} \times 100\% \quad [1]$$

where M represents the initial fluorine and chlorine content in zinc oxide dust, M' denotes the F and Cl content after roasting, and η represents the F and Cl removal efficiency.

Mechanism

In the conventional roasting process, the increase in temperature converts volatile halides into a gas phase, enabling their removal from the solid matrix. The removal of halides from zinc oxide dust by this high-temperature volatilization reaction is calculated using Equation [2].

The XRD analysis in Figure 2 shows that Zn existed mainly in the ZnO phase, while Pb existed mainly in the PbO and PbS phases. At high temperature, PbS reacts with O_2 in air and produces PbO and SO_2, which provides the necessary reactant for the sulphating reaction. In the sulphating roasting, water vapour carried by air was added to the microwave roasting process to strengthen the halide thermal hydrolysis reaction (Equation [3]) and sulphate reaction (Equation [4]), in order to further reduce the reaction temperature, shorten the reaction time, and improve the removal efficiency of F and Cl. The reactions are:

$$MeX_2 = MeX_2\,(g) \quad [2]$$

$$MeX_2 + H_2O = MeO + 2HX\,(g) \quad [3]$$

$$MeX_2 + H_2O + 1/2O_2 + SO_2 = MeSO_4 + 2HX\,(g) \quad [4]$$

where Me represents Pb^{2+} and Zn^{2+} and X denotes F^- and Cl^-.

Table II shows the Gibbs free energies (kJ·mol^{-1}) of the Pb and Zn halide thermal hydrolysis reactions and the sulphate reactions in the temperature range 600–900°C. Table III shows the equilibrium constants of the Pb and Zn chloride chemical reactions in the range 600–800°C. Tables II and III show that the Gibbs free energy of the sulphate reaction is at its minimum and equilibrium constant is at its maximum, which means that sulphate reaction is thermodynamically most feasible. The Gibbs free energy increases gradually with the increase in temperature, and the reaction becomes difficult. Thus, the temperature of sulphate roasting does not need to be very high.

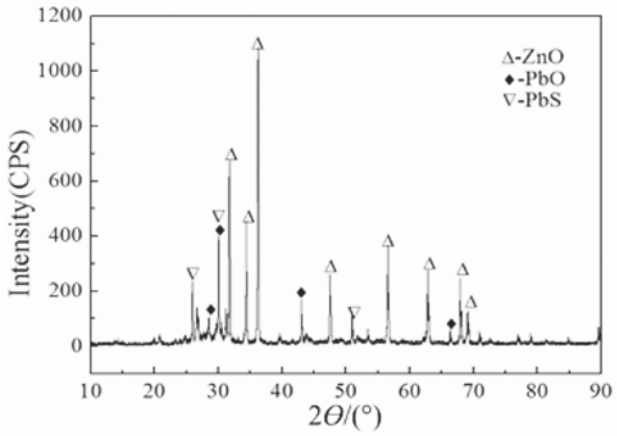

Figure 2—XRD patterns of zinc oxide dust sample

Table

Gibbs free energies (kJ·mol^{-1}) of Pb and Zn halides reaction

Matter	Volatile reaction				Thermal hydrolysis reaction				Sulphate reaction			
	873K	973K	1073K	1173K	873K	973K	1073K	1173K	873K	973K	1073K	1173K
$ZnCl_2$	3.76	0.91	-1.86	-4.54	27.44	18.65	18.27	21.38	-62.71	-43.79	-19.23	-9.31
$PbCl_2$	9.33	6.53	3.86	1.32	104.66	97.69	90.95	83.16	-67.90	-48.22	-27.36	-14.72
ZnF_2	26.47	22.61	18.8	15.12	0.33	-12.81	-25.77	-47.33	-89.82	-75.25	-63.27	-49.40
PbF_2	19.52	16.11	12.79	9.79	63.38	54.91	47.10	38.87	-109.28	-91.00	-71.20	-59.01

Table

Equilibrium constant of Pb and Zn halides reaction

Matter	Volatile reaction			Thermal hydrolysis reaction			Sulphate reaction		
	873K	973K	1073K	873K	973K	1073K	873K	973K	1073K
$ZnCl_2$	0.121	0.699	2.719	0.023	0.10	0.13	5651.63	224.45	8.63
$PbCl_2$	5.06×10^{-3}	3.67×10^{-2}	0.172	5.46×10^{-7}	5.52×10^{-6}	3.74×10^{-5}	1.16×10^{4}	387.78	21.46
ZnF_2	2.36×10^{-7}	8.35×10^{-6}	1.48×10^{-4}	0.960	4.870	17.980	2.37×10^{5}	1.10×10^{4}	1203.2
PbF_2	1.30×10^{-5}	2.41×10^{-4}	2.48×10^{-3}	1.61×10^{-4}	1.13×10^{-3}	5.09×10^{-3}	3.46×10^{6}	7.68×10^{4}	2.93×10^{3}

In a microwave field, the zinc oxide fume can be heated rapidly as a result of good microwave absorbance. The heating curves of 300 g of zinc oxide fume subjected to microwave power levels of 1200 W and 1800 W are plotted in Figure 3. The zinc oxide fume in a microwave field reaches 800°C within 8 minutes, which provides favourable thermodynamic and kinetic conditions for the removal of F and Cl by microwave sulphating roasting.

Method of analysis

The response surface methodology helps to optimize the effective parameters with a minimum number of experiments, and also analyses the interaction between the parameters and results (Azargohar and Dalai, 2005). Based on previous work, three influencing factors, namely the roasting temperature (X_1, °C), holding time (X_2, minutes), and vapour flow (X_3, ml/min), were considered independent variables.

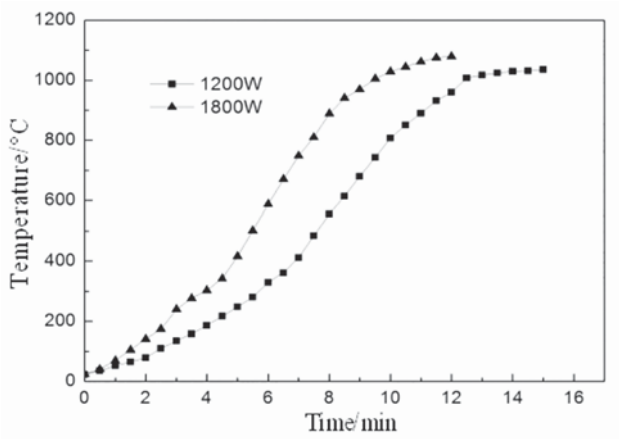

Figure 3—Heating behaviour of zinc oxide fume at different microwave powers

The dependent variables are the F and Cl removal efficiency from zinc oxide dust (Y_1, Y_2, %). Table IV shows the independent variables, experimental range, and levels of the design model. In order to describe the nature of the response surface in the optimum region, a central composite design with three coded levels was performed. In general, central composite designs need a total of (2^k +2k+N_0) runs where k is the number of factors studied, 2^k is the points from the factorial design, 2^k is the face-centered points, and N_0 is the number of experiments carried out at the centre.

Results and discussion

Response analysis and interpretation

The results of 20 runs of the CCD experiment are shown in Table V. The roasting temperatures of runs 9 and 10 were set as 566°C and 734°C, the holding times of runs 11 and 12 were set as 26 minutes and 94 minutes, and the vapour flows of runs 13 and 14 were set as 2.6 ml/min and 9.4 ml/min, respectively. The defluorination efficiency varied from 57.5% to 94.2% while the dechlorination efficiency varied from 53.5% to 93.4%.

The ANOVA results of the quadratic model for the defluorination efficiency and dechlorination efficiency are listed in Table VI and Table VII respectively. The model F-

Table

Experimental range and level of variables

Variables	Level code		
	-1	0	1
Roasting temperature X_1 (°C)	600	650	700
Holding time X_2 (min)	40	60	80
Vapour flow X_3 (ml/min)	4	6	8

Table

Central composite design arrangement and results

Run	Roasting temperature X_1 (°C)	Holding time X_2 (min)	Vapour flow X_3 (ml/min)	Defluorination efficiency Y_1 (%)	Dechlorination efficiency Y_2 (%)
1	600	40	4	57.7	53.5
2	700	40	4	74.3	65.9
3	600	80	4	79.0	71.0
4	700	80	4	92.8	90.6
5	600	40	8	66.8	61.7
6	700	40	8	85.0	77.6
7	600	80	8	81.7	76.0
8	700	80	8	94.2	93.4
9	565.9	60	6	71.6	63.5
10	734.1	60	6	90.6	88.7
11	650	26.4	6	60.1	53.0
12	650	93.6	6	92.4	90.7
13	650	60	2.6	80.5	74.6
14	650	60	9.4	93.0	91.2
15	650	60	6	88.6	85.8
16	650	60	6	88.0	86.5
17	650	60	6	87.5	86.1
18	650	60	6	88.2	85.6
19	650	60	6	89.6	85.0
20	650	60	6	88.7	85.5

Table

Defluorination efficiency analysis of variance for response surface quadratic model

Source	Sum of square	df	Mean square	F-value	P-value
Model	2263.21	9	251.47	62.99	< 0.0001
X_1	634.04	1	634.04	158.83	< 0.0001
X_2	1023.40	1	1023.40	256.37	< 0.0001
X_3	147.77	1	147.77	37.02	0.0001
X_1X_2	9.03	1	9.03	2.26	0.1635
X_1X_3	0.01	1	0.01	0.00	0.9587
X_2X_3	30.81	1	30.81	7.72	0.0195
X_1^2	130.99	1	130.99	32.81	0.0002
X_2^2	322.37	1	322.37	80.76	< 0.0001
X_3^2	14.91	1	14.91	3.74	0.0820
Residual	39.92	10	3.99	—	—

R_1^2=0.9827, $R_{1\,adj}^2$ = 0.9671

Table I

Dechlorination efficiency analysis of variance for response surface quadratic model

Source	Sum of square	df	Mean square	F-value	P-value
Model	3065.20	9	340.58	64.22	< 0.0001
X_1	849.04	1	849.04	160.09	< 0.0001
X_2	1348.44	1	1348.44	254.26	< 0.0001
X_3	226.50	1	226.50	42.71	< 0.0001
X_1X_2	9.46	1	9.46	1.78	0.2113
X_1X_3	0.21	1	0.21	0.04	0.8458
X_2X_3	18.30	1	18.30	3.45	0.0929
X_1^2	228.55	1	228.55	43.09	< 0.0001
X_2^2	433.56	1	433.56	81.75	< 0.0001
X_3^2	35.89	1	35.89	6.77	0.0264
Residual	53.03	10	5.30	—	—

R_2^2=0.9827, $R_{2\,adj}^2$ = 0.9677

value of 62.99 and 64.22 implies that the model is significant. There is only a 0.01% chance that this large model F-value could occur by chance. Values of 'Prob.> F' of less than 0.050 indicate that the model terms are significant (Myers and Anderson-Cook, 2009). In this case, X_1, X_2, X_3, X_1^2, and X_2^2 are the significant model terms. That is, among the three independent variables tested, the roasting temperature ($p < 0.0001$), holding time ($p < 0.0001$), and vapour flow ($p < 0.050$) have significant linear effects as well as quadratic effects on the defluorination and dechlorination efficiency. According to (Myers and Anderson-Cook (2009), for a good fit of a model, the correlation coefficient should be at least 0.80. The 'Pred R-squared' of 0.9827 is in reasonable agreement with the 'Adj R-squared' of 0.9671 plotted in the Table VI and Table VIII. Hence, the model can be used to navigate the design space.

The constants and coefficients were obtained by fitting the data listed in Table VI and Table VII in to Equation [5] and Equation [6] respectively. The equation in terms of coded factors is obtained.

$$Y_1=-654.79+1.77X_1+2.84X_2+7.40X_3-1.06E^{-3}X_1X_2+3.75\,E^{-4}X_1X_3-0.049X_2X_3-1.21E^{-5}X_1^2-0.0118X_2^2-0.254X_3^2 \quad [5]$$

$$Y_2=-760.14+2.15X_1+1.66X_2+7.98X_3+1.09E^{-3}X_1X_2+1.63E^{-3}X_1X_3-0.0378X_2X_3-1.59E^{-4}X_1^2-0.0137X_2^2-0.395X_3^2 \quad [6]$$

It is important to confirm that the selected model provides an adequate approximation to the real system. By using the diagnostic plots, including normal probability *vs.* Studentized residuals and the predicted *vs.* actual value, the model adequacy can be judged (Myers and Anderson-Cook, 2009; Joglekar and May, 1987).

Figure 4 shows the normal probability plots of the Studentized residuals for the initial discharge capacity. The normal probability plot indicates that the residuals follow a normal distribution and the points follow a straight line, verifying that the model is valid and gives a plausible fit to the experimental data.

As seen in Figure 5, the actual response values are the experimental data for a particular run, and the predicted response values are evaluated by the approximating functions. The predicted values are in good agreement with the experimental values, indicating that the model is valid and successfully fits the experimental data.

Response surface

To achieve a better understanding of the interactions of the variables and to determine the optimum level of each variable for the maximum dechlorination efficiency of zinc oxide dust, three-dimensional response surfaces plots of the relationship between X_1 and X_2, X_1 and X_3, and X_2 and X_3 were calculated

Table

Optimization process parameters of regression model

Roasting temperature X_1 (°C)	Holding time X_2 (min)	Vapour flow X_3 (ml/min)	Defluorination efficiency Y_1 (%)		Dechlorination efficiency Y_2 (%)	
			Predicted	Experimental	Predicted	Experimental
655	65.2	6.8	92.0	91.3	90.0	89.5

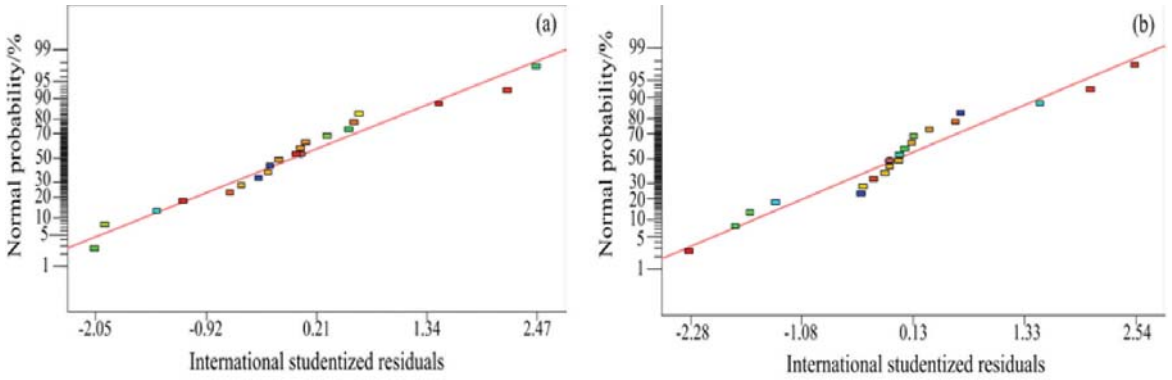

Figure 4—(a) Defluorination efficiency and (b) dechlorination efficiency: normal probability plots of Studentized residuals

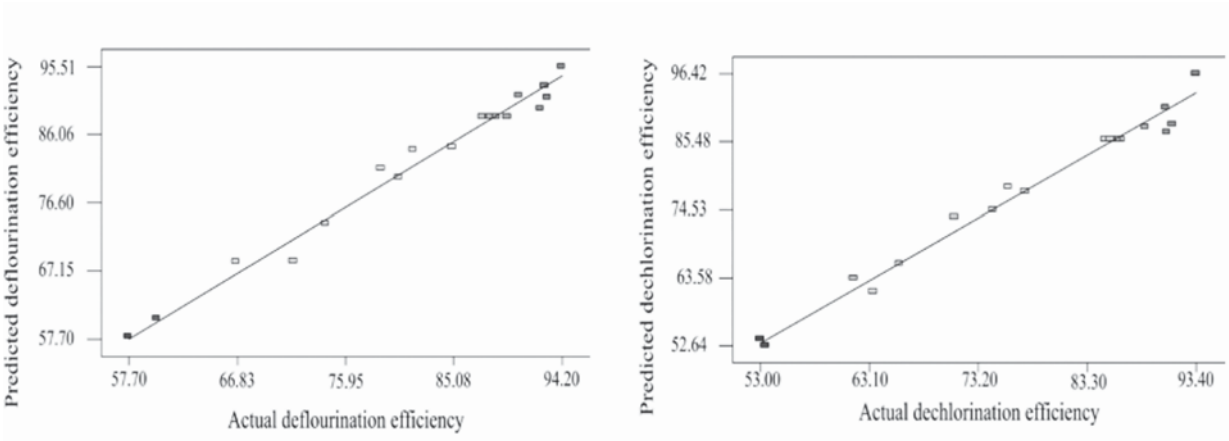

Figure 5—Linear correlation between (a) actual and (b) predicted defluorination efficiency and dechlorination efficiency

and are illustrated in Figure 7. X_1, X_2, and X_3 were held constant at their average values. The figures are constructed to assess the interactive relationships between the independent variables and the response.

Figure 7(a) and (d) show the defluorination and dechlorination efficiency of zinc oxide dust as a function of the roasting temperature and holding time, with the water vapour flow kept constant (6 ml/min). The roasting temperature has a significant positive effect on defluorination and dechlorination efficiency. The efficiency increased quickly as the roasting temperature increased. According to different Gibbs free energies of the selected three reactions (Table II), the sulphate reaction is easiest to carry out in this microwave sulphating roasting process. The higher equilibrium constant of the sulphate at elevated temperatures (Table III) indicates that the sulphate reaction is exothermic. Figure 6 shows that the PbS phase disappears in the roasting process. The oxidation of PbS is also exothermic. An appropriate roasting temperature is important to the sulphate reaction. The defluorination and dechlorination efficiency is therefore substantial at 600°C, with a further significant increase when the reaction temperature is increased to 700°C.

As shown in Figure 7(b) and (e), the defluorination and dechlorination efficiency increased with the vapour flow, but compared with roasting temperature, the vapour flow has a smaller effect on the defluorination and dechlorination efficiency. The defluorination and dechlorination efficiency was controlled by the diffusion at a certain temperature. The reaction interface increased with an increase in the vapour flow rate, and a larger solid-gas interface improves the defluorination and dechlorination efficiency significantly.

Figure 7(c) and (f) show the effect of the holding time and the vapour flow on the defluorination and dechlorination efficiency for a constant roasting temperature. The defluorination and dechlorination efficiency increased with an increase in the holding time. Compared to the vapour flow rate, the holding time has a more significant effect on the efficiency. With substantial holding time, the residual F and Cl levels in zinc oxide fume are further reduced, with the optimum removal efficiency stabilizing at a certain temperature and vapour flow.

Optimal conditions and verification of model

The aim of this study was to investigate the values of the three operational parameters (roasting temperature, holding time, and vapour flow) that maximize the defluorination and dechlorination efficiencies, using response surface methodology. The experimental values were compared with those predicted in order to determine the validity of the model.

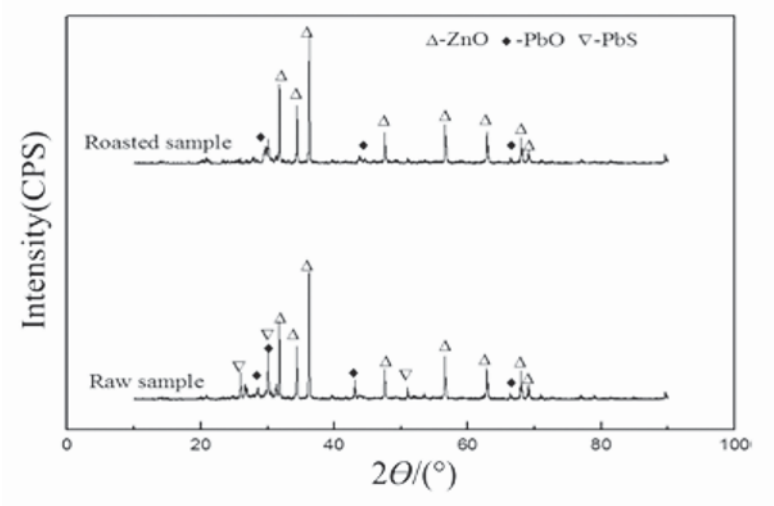

Figure 6—XRD patterns of raw sample and roasted sample of zinc oxide fume

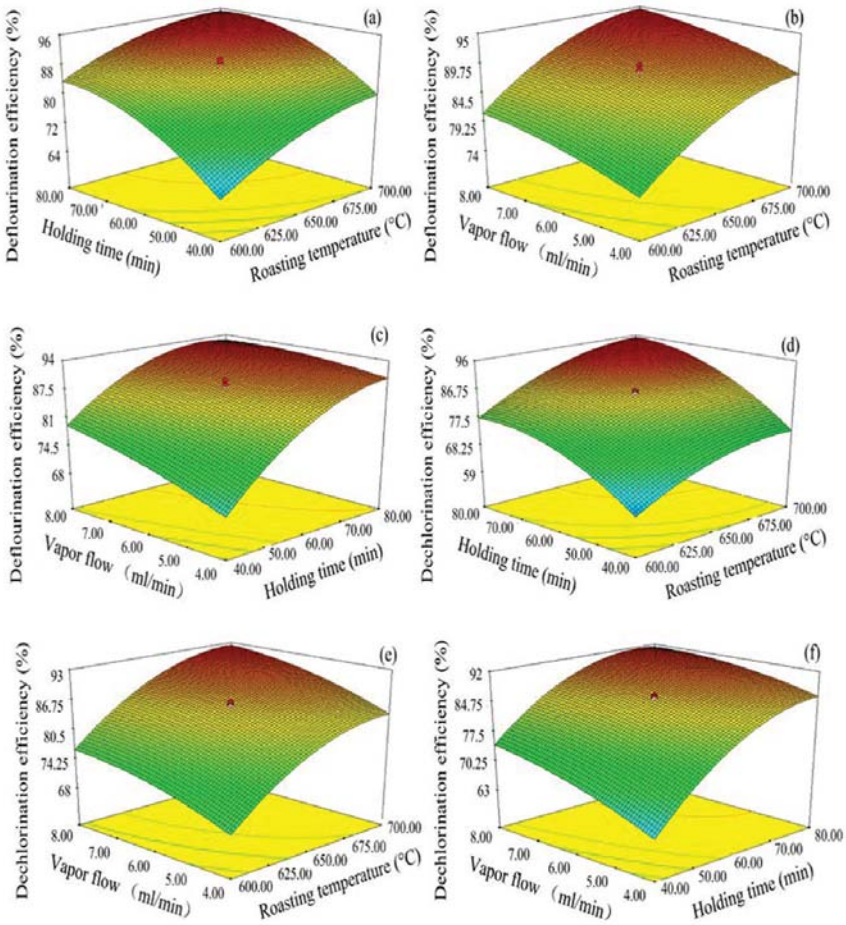

Figure 7—Response surface plots of defluorination efficiency for (a) roasting temperature vs holding time, (b) roasting temperature vs vapour flow (c) holding time vs vapour flow, and dechlorination efficiency for (d) roasting temperature vs holding time, (e) roasting temperature vs vapour flow, (f) holding time vs vapour flow

From the model, optimized conditions were obtained and are given in Table VIII. The optimum levels of the three variables were found to be a roasting temperature of 655°C, holding time of 65.2 minutes, and vapour flow at 6.8 ml/min with a prediction of 92.0% for the defluorination efficiency and 90.0% for the dechlorination efficiency. In order to test the validity of the optimum conditions obtained by the empirical model, a confirmatory experiment was carried out

using these optimal levels. The actual experimental value of defluorination efficiency is 91.3% with a relative error of 0.76% with respect to the predicted value, while the actual experimental value of dechlorination efficiency is 89.5% with a relative error of 0.56%. This indicates that the experimental values are in agreement with the predicated ones. The F and Cl contents of the roasted sample were measured as 14.5 mg/L and 15.3 mg/L respectively, satisfying the requirements (F < 80 mg/L, Cl < 100 mg/L) in the zinc electrolysis process.

Conclusions

1. The response surface methodology showed that it is feasible to removal the fluorides and chlorides from zinc oxide dust from a zinc fuming furnace by microwave sulphating roasting
2. The dechlorination efficiency is significantly affected by roasting temperature and holding time, and to a lesser degree by vapour flow rate
3. The optimized calcination conditions are as follows: roasting temperature 655°C, holding time 65.2 minutes, and vapour flow rate 6.8 ml/min. The defluorination and dechlorination efficiencies are 92.6% and 90.2% respectively, which agree well with the experimental values of 91.3% and 89.5% under the optimized conditions, suggesting that regressive equation fits the defluorination and dechlorination efficiencies perfectly
4. The F and Cl contents of the roasted sample under the conditions predicted by RSM were reduced to 14.5 mg/L and 15.3 mg/L respectively, satisfying the requirements in the zinc electrolysis process.

Acknowledgements

The authors are grateful for the financial support from the National Natural Science Foundation (No. 51104073), the National Technology Research and Development Program of China (No. 2013AA064003), the Yunnan Province Young Academic Technology Leader Reserve Talents (2012HB008), and Yunnan Provincial Science and Technology Innovation Talents scheme – Technological Leading Talent (No. 2013HA002).

References

Agrawal, A., Sahu, K.K., and Pandey, B.D. 2004. Recent trends and current practices for secondary processing of zinc and lead. Part I: lead recovery from secondary sources. *Waste Management and Research*, vol. 22. pp. 240–247.

Azargohar, R. and Dalai, A. 2005. Production of activated carbon from Luscar char: experimental and modeling studies. *Microporous and Mesoporous Materials*, vol. 85. pp. 219–225.

Barakat, M. 2003. The pyrometallurgical processing of galvanizing zinc ash and flue dust. *JOM*, vol. 55. pp. 26–29.

Cinar Sahin, F., Derin, B., and Y Cel, O. 2000. Chloride removal from zinc ash. *Scandinavian Journal of Metallurgy*, vol. 29. pp. 224–230.

D'heilly, J., Sun, Z., Wen, X., and West, S. 2007. Fluoride ion selective electrode. US patent 20070199816 A1.

Dakhili, N., Razavizadeh, H., Salehi, M., and Seyedein, S.H. 2011. Recovery of zinc from the final slag of steel's galvanizing process. *Advanced Materials Research*, vol. 264. pp. 592–596.

Gresin, N. and Topkaya, Y. 1998. Dechlorination of a zinc dross. *Hydrometallurgy*, vol. 49. pp. 179–187.

Jha, M.K., Kumar, V., and Singh, R.J. 2001. Review of hydrometallurgical recovery of zinc from industrial wastes. *Resources, Conservation and Recycling*, vol. 33. pp. 1–22.

Joglekar, A. and May, A. 1987. Product excellence through design of experiments. *Cereal Foods World*, vol. 32. pp. 857–868.

Lan, Y., Zhao, Q., and Smith, R. 2006. Recovery of zinc from high fluorine bearing zinc oxide ore. *Mineral Processing and Extractive Metallurgy*, vol. 115. pp. 117–119.

Lashgari, M. and Hosseini, F. 2013. Lead-silver anode degradation during zinc electrorecovery process: chloride effect and localized damage. *Journal of Chemistry*, vol. 2013. Article ID 538462. DOI 10.1155/2013/538462

Li, M., Peng, B., Chai, L., Peng, N., Yan, H., and Hou, D. 2012. Recovery of iron from zinc leaching residue by selective reduction roasting with carbon. *Journal of Hazardous Materials*, vol. 237. pp. 323–330.

Myers, R.H. and Anderson-Cook, C.M. 2009. Response Surface Methodology: Process and Product Optimization using Designed Experiments. Wiley, New York.

Sahu, K.K., Agrawal, A., and Pandey, B.D. 2004. Recent trends and current practices for secondary processing of zinc and lead. Part II: zinc recovery from secondary sources. *Waste Management and Research*, vol. 22. pp. 248–254.

Vahidi, E., Rashchi, F., and Moradkhani, D. 2009. Recovery of zinc from an industrial zinc leach residue by solvent extraction using D2EHPA. *Minerals Engineering*, vol. 22. pp. 204–206.

Wang, C., Hu, X., Matsuura, H., and Tsukihashi, F. 2007. Evaporation kinetics of the molten $PbCl_2$-$ZnCl_2$ system from 973 to 1073 K. *ISIJ international*, vol. 47. pp. 370–376.

Zeng, Z-G., Dou, C-L., Liu, W-P., Xi, X-M., and Xiao, S-W. 2007. Measures to reinforce the de-halogen roasting of zinc oxide dust in multi-hearth furnace. *Mining and Metallurgical Engineering*, 2007–01.

Zenki, M. and Iwadou, Y. 2002. Repetitive determination of chloride using the circulation of the reagent solution in closed flow-through system. *Talanta*, vol. 58. pp. 1055–1061. ◆